# Bonding, Hyperfine Interactions, and Lattice Dynamics of Cationic and Neutral Ferrocenyl-Substituted Allylic and Cumulenic Compounds

**Rolfe H. Herber,*,† Benno Bildstein,‡ Peter Denifl,‡ and Herwig Schottenberger‡**

Racah Institute of Physics, The Hebrew University, 91904 Jerusalem, Israel, and Institut fur Allgemeine, Anorganische, und Theoretische Chemie, Universität Innsbruck, Innrain 52a, A-6020 Innsbruck, Austria

*Received November 27, 1996*[⊗]

The synthesis and spectroscopic characterization (by mass, UV−visible, IR, NMR and $^{57}$Fe Mössbauer spectroscopy) of three new compounds related to seven recently published ferrocenyl-substituted allylic and cumulenic compounds are reported and have made it possible to effect a systematic evaluation of the parameters extractable from temperature-dependent $\gamma$ ray resonance studies. For the neutral species, the hyperfine parameters (IS and QS) of the $\sigma$-bonded ferrocenyl groups are insensitive to the structural details of the allylic or cumulenic carbon framework. The temperature dependence of the recoil-free fraction is dominated by the Cp ring−iron atom interaction, and is not diagnostic of the detailed molecular architecture. In the case of the carbocationic complexes, two distinct iron sites are resolvable from the Mössbauer data. The detailed temperature-dependent behavior of the hyperfine parameters and recoil-free fraction for 10 complexes with either equivalent termini, linked by similar, but different types of bridges (neutral **1**−**5**), or with inequivalent moieties linked by related or identical connectors (cationic **6**−**10**), has been elucidated over the temperature range $90 \le T \le 300$ K. An X-ray crystallographic study of (*R*,*S*)-ferroceno[2,3-*a*]inden-1-one proved the racemic nature of this progenitor of compound **10**: monoclinic, $P2_1/c$, $a = 9.29.3(2)$ pm, $b = 1083.7(2)$ pm, $c = 1345.7(3)$ pm, $\beta = 108.41(3)$, $V = 1.2859(5)$ nm$^3$, $Z = 4$, $R(F_o) = 0.0574$, $R_w$ $(F_o^2) = 0.1394$.

## Introduction

It was recognized soon after the correct characterization of the structure and bonding in ferrocene[1] and ferricinium complexes[2] that metallocenes are among the most efficient carbenium stabilizing groups,[3] serving as donor moieties for satisfying the electron deficiency of the α-carbenium fragment. The chemistry of such systems has been thoroughly investigated,[4] including conjugated allylium and allenylium representatives.[5] Formally, neutral perferrocenylated cumulenes[6] are related to these cationic species by introduction of an additional anionic ferrocene substituent. Besides ferrocene-stabilized carbenium ions, dinuclear metal-stabilized propargylic carbocations are known[7] with the isolobal metal carbonyl cluster fragments $Cp_2Mo_2(CO)_4$, $Cp_2W_2(CO)_4$, and $Co_2(CO)_6$ as donors, and in a few cases "mixed" cationic systems with a metal carbonyl fragment and with a ferrocenyl group have been reported.[8]

Taken together, these ferrocenylated olefins, cumulenes, and allylic, cumulenic, and propargylic cations represent a closely related set of compounds, allowing the comparison and/or evaluation of their physical properties. Due to the presence of the iron atom(s) in such ferrocenyl-substituted cationic or neutral hydrocarbons, $^{57}$Fe Mössbauer spectroscopy offers an additional insight into the nature of these complexes, and several previous studies on related organometallics using this technique have been reported.[9,10] Much of the attention in these Mössbauer investigations has centered on the determination of the hyperfine interaction parameters, particularly the isomer shift (IS) and quadrupole splitting (QS), since these are most readily extracted from the spectroscopic data. In addition, however, the deter-

† The Hebrew University.
‡ Universität Innsbruck.
[⊗] Abstract published in *Advance ACS Abstracts,* July 15, 1997.

(1) Dahl, J. P.; Ballhausen, C. F. *Mat. Fys. Medd. K. Dan. Vidensk. Selsk.* **1961**, *33* (5). See also the discussion in: *Gmelin Handbuch Der Anorganischen Chemie*; Springer Verlag: Berlin, 1974; Vol. 14A, pp 15 ff, and references therein. Crabtree, R. H. *The Organometallic Chemistry of the Transition Metals*, 2nd ed.; Wiley and Sons: New York, 1994, and references therein. Rosenblum, M. *Chemistry of the Iron Group Metallocenes*; Interscience Publishers: New York, 1965; Part I, and references therein. Coates, G. E. *Organometallic Compounds*; Methuen and Co.: London, 1960; pp 237 ff, and references therein.

(2) Collins, R. L. *J. Chem. Phys.* **1965**, *42*, 1072. See also the discussion in: Greenwood, N. N.; Gibb, T. C. *Mossbauer Spectroscopy*; Chapman Hall: London, 1971; pp 233 ff.

(3) Hill, E. A.; Richards, S. H. *J. Am. Chem. Soc*. **1959**, *81*, 3483. Cais, M. *Organomet. Chem. Rev.* **1966**, *1*, 435.

(4) Watts, W. E. In *Comprehensive Organometallic Chemistry*; Wilkinson, G., Stone, F. G. A., Abel, E. W., Eds.; Pergammon Press: Oxford, UK, 1982; Vol. 8, Chapter 59, pp 1051 ff.

(5) Lukasser, J.; Angleitner, H.; Schottenberger, H.; Kopacka, H.; Schweiger, M.; Bildstein, B.; Ongania, K.-H.; Wurst, K. *Organometallics* **1995**, *14*, 5566, and references therein.

(6) Bildstein, B.; Denifl, P.; Wurst, K.; Andre, M.; Baumgarten, M.; Friedrich, J.; Ellmerer-Müller, E. *Organometallics* **1995**, *14*, 4334. Bildstein, B.; Kopacka, H.; Schweiger, M.; Ellmerer-Müller, E.; Ongania, K.-H.; Wurst, K. *Organometallics* **1996**, *15*, 4398. Bildstein, B.; Kopacka, H.; Schweiger, M.; Wurst, K. Presented at the 211th National Meeting of the American Chemical Society, New Orleans, LA, March 24−28, 1996.

(7) Melikyan, G. G.; Nicholas, K. M. In *Modern Acetylene Chemistry*; Stang, P. J., Diederich, F., Eds.; VCH: New York, 1995. Amouri, H. E.; Gruselle, M. *Chem. Rev.* **1996**, *96*, 1077.

(8) Cordier, C.; Gruselle, M.; Vaissermann, J.; Troitskaya, L. L.; Bakhmtov, V. I.; Sokolov, V. I.; Jaouen, G. *Organometallics* **1992**, *11*, 3825. Capon, J.-F.; Le Berre-Cosquer, N.; Kergoat, R. *J. Organomet. Chem.* **1996**, *508*, 1. Capon, J.-F.; Le Berre-Cosquer, N.; Leblanc, B.; Kergoat, R. *J. Organomet. Chem.* **1996**, *508*, 31. Troitskaya, L. L.; Sokolov, V. I.; Bakhmutov, V. I.; Reutov, O. A.; Gruselle, M.; Cordier, C.; Jaouen, G. *J. Organomet. Chem.* **1989**, *364*, 195.

(9) Watanabe, M.; Iwamoto, T.; Nakashima, S.; Sakai, H.; Motoyama, I.; Sano, H. *J. Organomet. Chem.* **1993**, *448*, 167. Neshvad, G.; Roberts, R. G. M.; Silver, J. *J. Organomet. Chem.* **1982**, *236*, 237. Houlton, A.; Miller, R. J.; Roberts, R. G. M.; Silver, J. *J. Chem Soc., Dalton Trans.* **1990**, 2181.

(10) (a) Houlton, A.; Miller, R. J.; Roberts, R. G. M.; Silver, J. *J. Chem. Soc., Dalton Trans.* **1991**, 467, and references therein. (b) Herber, R. H.; Hanusa, T. P. *Hyperfine Interactions* **1997**, *108*, 563. (c) Webb, R. J.; Lowery, M. D.; Shiomi, Y.; Sorai, M.; Wittebort, R. J.; Hendrickson, D. N. *Inorg. Chem.* **1992**, *31*, 5211. (d) Webb, R. J.; Hagen, P. M.; Wittebort, R. J.; Sorai, M.; Hendrickson, D. N. *Inorg. Chem.* **1992**, *31*, 1791, and references therein.

S0020-1669(96)01422-X CCC: $14.00 

mination of the temperature dependence of these parameters, and more importantly, the temperature dependence of the recoil-free fraction of the metal atom in these compounds, can serve to shed additional light on the behavior of the (distinguishable) ferrocenyl groups. In this context, in the detailed Mössbauer and crystallographic study of ferrocenium hexafluorophosphate, Hendrickson *et al.*[10c] made use of the temperature dependence of the recoil-free fraction to identify the several phase transitions (phase IV below 211 K, and phase II in the temperature range up to 347 K) in this solid and correlated these with the crystallographic order parameters. It should be noted, however, that this cationic iron center gives rise to relaxation spectra consisting of a (broad) single resonance, rather than the doublet spectra of the present study. Similarly, in an earlier study, Hendrickson *et al.*[10d] monitored the phase transitions in mixed-valent biferrocenes, using similar temperature-dependent $^{57}$Fe Mössbauer effect techniques, by elucidating the $T$ dependence of the QS hyperfine parameter over the temperature range $4.2 \leq T \leq 300$ K.

The application of such techniques, focusing in particular on the dynamical behavior of the metal centers, is the subject of the present investigation. Moreover, the use of ferrocene (and ferrocenyl ligands) as probes for the dynamical behavior of other molecular systems, such as $C_{60}$ [11] has been suggested by a number of investigators,[12] and the present study addresses the validity of the use of ferrocene-related materials as "reporter" moieties in such studies.

## Experimental Section

**Synthesis.** Tetraferrocenylethane **1**,[6,13] -ethylene **2**,[6] -allene **3**,[6] and -butatriene **4**;[14] triferrocenylallenylium tetrafluoroborate **5**,[5] and triferrocenylpentatetraenylium tetrafluoroborate **6**;[14] and cyclopentadienyl-(1,3-diferrocenyl-1-ylium)iron tetrafluoroborate **7**[5] have been prepared as published recently[5,6] and a full account of the synthesis and chemical properties of **4** and **6** is in preparation.[14] General procedures and specific analytical instrumentation have been published elsewhere.[5] The syntheses of **8**−**10** are summarized in Scheme 1 and given in detail below.

**$Co_2(CO)_6${cyclopentadienyl($\mu$-$\eta^2$:$\eta^2$-1-(ferrocenylethynyl)-3-ferrocenyl-1-ylium)iron} Tetraphenylborate (8).** In analogy to the synthesis of **7**,[5] a Schlenk vessel was charged with 527 mg of ethynylferrocene[15] (2.51 mmol, 1.32 mequiv with regard to cyclopentadienyl(3-ferrocenyl-1-oxypentalenyl)iron[16]) and 30 mL of THF at −60 °C. After addition of 2.27 mL of a 1.0 M solution of methyllithium in *n*-hexane/ether (2.27 mmol), the mixture was allowed to warm to room temperature. To the so-formed solution of (ferrocenylethynyl)lithium was added 800 mg (1.89 mmol) of cyclopentadienyl(3-ferrocenyl-1-oxypentalenyl)iron[16] in one portion and the mixture was stirred at room temperature overnight. The resulting solution of the alcoholate was hydrolyzed with the minimal amount of $H_2O$, the THF solution of the alcohol was dried with $Na_2SO_4$ and filtered rapidly, and the solvent was removed in vacuo, yielding crude cyclopentadienyl(1-(ferrocenylethynyl)-1-hydroxy-3-ferrocenylpentalenyl)iron, which was used without further purification because of its limited stability.

After the crude alcohol was dissolved in 50 mL of dry, deoxygenated THF, 950 mg (2.77 mmol) of $Co_2(CO)_8$ was added under an atmosphere of argon and the mixture was stirred at room temperature for 2 h, during which time the evolution of CO indicated complexation. THF was removed in vacuo, the residue was dissolved in ether, insoluble materials were filtered off, and the solution was evaporated to dryness on a rotary evaporator. The residue was dissolved in 20 mL of glacial acetic acid, and 0.25 mL (2.83 mmol) of triflic acid was added to effect dehydration and cation formation. After stirring for 10 min, a solution of 0.415 g of sodium tetraphenylborate in 3 mL of acetic acid was added, the mixture was stirred for 15 min, and the precipitated product was filtered off, washed with four portions of acetic acid, one portion of ether, and six portions of *n*-hexane, and dried in vacuo, yielding 0.96 g (42% with regard to the starting ketone) of $Co_2(CO)_6${cyclopentadienyl($\mu$-$\eta^2$:$\eta^2$-1-(ferrocenylethynyl)-3-ferrocenyl-1-ylium)iron} tetraphenylborate (**8**) as a dark green microcrystalline solid: mp 99−101 °C (dec). Anal. Calcd for $C_{65}H_{47}Fe_3O_6Co_2B$: C, 63.98; H, 3.88. Found: C, 63.79; H, 3.92. HRMS (FAB): *m/z* 900.835 20 ($M^+$ of cation; exact mass calcd for $C_{41}H_{27}Fe_3O_6Co_2$ 900.851 95). MS (EI, 70 eV): *m/z* 901 (81) ($M^+$ of cation), 873 (43) ($M^+ - CO$), 817 (54) ($M^+ - 3CO$), 789 (100) ($M^+ - 4CO$), 761 (88) ($M^+ - 5CO$), 733 (83) ($M^+ - 6CO$), 674 (24) ($M^+ - (CO)_6Co$), 615 (32) ($M^+ - (CO)_6Co_2$). UV−visible ($CH_2Cl_2$; $\lambda_{max}$ (nm)/log $\epsilon$): 397/3.95, 636/3.61, 896/3.83. IR (KBr): 3098 w, 3054 w, 2983 w, 2087 s, 2054 s, 2025 s, 1622 w, 1580 w, 1524 m, 1472 w, 1437 w, 1408 w, 1107 w, 1030 w, 1001 w, 821 m, 733 m, 704 m, 611 w, 511 m, 493 m, 466 m cm$^{-1}$. Attempted NMR analysis gave inconclusive results, only broad signals due to paramagnetic impurities were observed (compare Mössbauer data).

**$Cp_2Mo_2(CO)_4${cyclopentadienyl($\mu$-$\eta^2$:$\eta^2$-1-(ferrocenylethynyl)-3-ferrocenyl-1-ylium)iron} Tetrafluoroborate (9).** Crude cyclopentadienyl(1-(ferrocenylethynyl)-1-hydroxy-3-ferrocenylpentalenyl)iron was prepared from 700 mg (1.7 mmol) of cyclopentadienyl(3-ferrocenyl-1-oxypentalenyl)iron[16] by a procedure analogous to that described for **8** and was stirred with $[Cp_2Mo_2(CO)_4]$[17] at room temperature for 24 h; the resulting alcohol complex was converted to the cation with tetrafluoroboric acid and worked-up in a manner similar to that described for **8**, yielding 783 mg (41.5% based on starting ketone) of $Cp_2Mo_2(CO)_4${cyclopentadienyl($\mu$-$\eta^2$:$\eta^2$-1-(ferrocenylethynyl)-3-ferrocenyl-1-ylium)iron} tetrafluoroborate (**9**) as a dark green microcrystalline solid: mp not observed, decomposition without melting. Anal. Calcd for $C_{48}H_{37}Fe_3O_4Mo_2BF_4$: C, 51.29; H, 3.32. Found: C, 51.12; H, 3.35. MS (EI, 70 eV or FAB): molecular ion of cation with $m/z$ = 1049 was not observed. UV−visible ($CH_2Cl_2$; $\lambda_{max}$ (nm)/log $\epsilon$): 846/3.8. IR (KBr): 3108 m, 1989 s, 1958 s, 1900 m, 1890 m, 1638 w, 1528 m, 1443 m, 1414 m, 1354 w, 1107 s, 1084 s, 1047 s, 1005 m, 924 w, 825 s, 480 m cm$^{-1}$. $^1$H NMR ($CD_2Cl_2$): $\delta$ 4.16, 4.23, 4.39 (each signal 5H, s, unsubstituted Cp); 5.26 (10H, br s, 2 × unsubstituted Cp); 4.60, 4.64, 4.71, 4.79, 5.37, 5.79, 6.30, 6.38, 6.55 (12H, each signal broad pseudo s, substituted Cp). No $^{13}$C NMR spectrum could be obtained due to decomposition in solution during accumulation of the FID.

**(*R*,*S*)-Ferroceno[2,3-*a*]inden-1-ferrocenyl-1-ylium tetrafluoroborate (10).** A Schlenk vessel was charged with 406 mg (2.98 mmol) of ferrocenyl lithium[18] and 30 mL of dry, deoxygenated ether. After external cooling the suspension to −60 °C, 773 mg (2.68 mmol) of (*R*,*S*)-ferroceno[2,3-*a*]inden-1-one[19] was added in one portion with protection from air. The cooling bath was removed, and the mixture was stirred at ambient temperature overnight. After aqueous workup and extraction with ether, the crude (*R*,*S*)-ferroceno[2,3-*a*]inden-1-ferrocenyl-1-ol was converted to the corresponding tetrafluoroborate in a manner similar to that described for **8** or **9**, yielding 661 mg (45.3%)


(11) Crane, D. J.; Hitchcock, P. B.; Kroto, H. W.; Taylor, R.; Walton, D. R. M. *J. Chem. Soc., Chem. Commun.* **1992**, 1764.

(12) Kucharski, Z.; Byszewski, P.; Suwalski, J. *Mater. Sci. Forum* **1995**, *191*, 31. Byszewski, P.; Diduszko, R.; Kowalska, E. *Proc. Electrochem. Soc.* **1994**, *94-24*, 1392−1401 (Recent Advances in the Chemistry of Fullerenes and Related Materials). Kucharski, Z., private communication to R.H.H. Gibb, T. C. *J. Phys. C, Solid State* **1976**, 2627. See also: Herber, R. H. *Acc. Chem. Res.* **1982**, *15*, 216, and references therein.

(13) Paulus, H.; Schlögl, K.; Weissensteiner, W. *Monatsh. Chem.* **1982**, *113*, 767. Sato, M.; Asai, M. *J. Organomet. Chem.* **1992**, *430*, 105.

(14) Bildstein, B.; et al., to be published.

(15) Wurst, K.; Elsner, O.; Schottenberger, H. *Synlett* **1995**, *8*, 833, and references cited therein.

(16) Abram, T. S.; Watts, W. E. *J. Chem. Soc., Perkin Trans. 1* **1977**, 1527. Egger, H.; Schlögl, K. *Monatsh. Chem.* **1964**, *95*, 1750.

(17) Curtis, M. D.; Fotinos, N. A.; Messerle, L.; Sattelberger, A. P. *Inorg. Chem.* **1983**, *22*, 1559.

(18) Guillaneux, D.; Kagan, H. B. *J. Org. Chem.* **1995**, *60*, 2502. Rebiere, F.; Samuel, O.; Kagan, H. B. *Tetrahedron Lett.* **1990**, *31*, 3121. Sanders, R.; Mueller-Westerhoff, U. T. *J. Organomet. Chem.* **1996**, *512*, 219. Buchmeiser, M.; Schottenberger, H. *J. Organomet. Chem.* **1992**, *436*, 223.

(19) Cais, M.; Modiano, A.; Raveh, A. *J. Am. Chem. Soc.* **1965**, *87*, 5607. Lehner, H.; Schlögl, K. *Monatsh. Chem.* **1970**, *101*, 895. Schottenberger, H.; Buchmeiser, M.; Elsner, O.; Ernst, E.; Reussner, J.; Neissl, W.; Angleitner, H. U.S. Pat. 5,521,265 (PCD Polymere Ges.m.b.H.) May 28, 1996.

**Table 1.** Crystallographic Data for (*R*,*S*)-Ferroceno[2,3-*a*]inden-1-one

| | |
|---|---|
| chemical formula | $C_{17}H_{12}FeO$ |
| formula weight | 288.12 |
| space group | monoclinic $P2_1/c$ |
| $a$ | 929.3(2) pm |
| $b$ | 1083.7(2) pm |
| $c$ | 1345.7(3) pm |
| $\beta$ | 108.41(3)° |
| $V$ | 1.2859(5) nm$^3$ |
| $Z$ | 4 |
| $T$ | 293 K |
| $\lambda$ | 71.073 pm |
| $\rho_{calcd}$ | 1.488 g cm$^{-3}$ |
| $\mu$ | 1.159 mm$^{-1}$ |
| R1[a] | 0.0574 |
| wR2[b] | 0.1394 |

[a] $R1 = \sum||F_o| - |F_c||/\sum|F_o|$. [b] $wR2 = [\sum[w(F_o^2 - F_c^2)^2]/\sum[w(F_o^2)^2]]^{1/2}$.

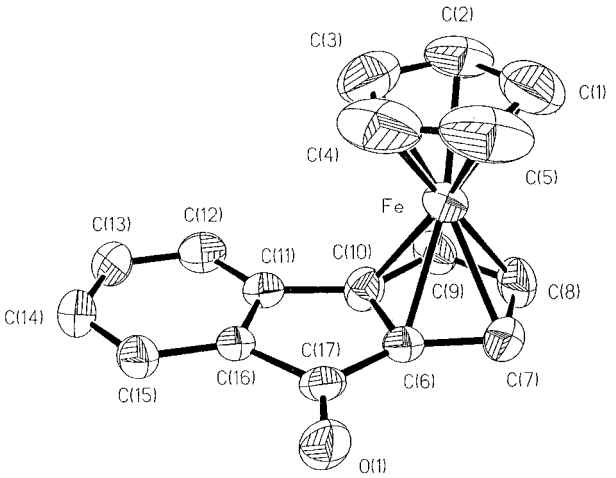


**Figure 1.** ORTEP drawing of (*R*,*S*)-ferroceno[2,3-*a*]inden-1-one. Ellipsoids are drawn at the 50% probability level, and hydrogen atoms are omitted for clarity.

of (*R*,*S*)-ferroceno[2,3-*a*]inden-1-ferrocenyl-1-ylium tetrafluoroborate (**10**) as dark green microcrystalline powder: mp not observed, up to 330 °C no melting or decomposition. Anal. Calcd for $C_{27}H_{21}Fe_2BF_4$: C, 54.07; H, 3.53. Found: C, 54.19; H, 3.54. HRMS (FAB): *m*/*z* 457.046 44 ($M^+$ of cation; exact mass calcd for $C_{27}H_{21}Fe_2$ 457.034 19). MS (EI, 70 eV): *m*/*z* 457 (100) ($M^+$ of cation), 392 (28) ($M^+ - Cp$), 336 (83) ($M^+ - 3CpFe$), 215 (36) ($M^+ - CpFe - CpFe$). UV−visible ($CH_2Cl_2$; $\lambda_{max}$ (nm)/log $\epsilon$): 268/4.22, 393/4.16, 800/3.94. IR (KBr): 3102 w, 1603 m, 1513 vs, 1445 m, 1414 m, 1391 w, 1341 w, 1107 m, 1068 s, 1036 s, 937 w, 829 m, 754 w, 712 s, 677 w, 567 w, 520 w, 507 m, 480 m, 451 w, 420 w cm$^{-1}$. $^1$H NMR ($CD_2Cl_2$): $\delta$ 4.42 (5H, s, unsubstituted Cp), 4.54 (5H, s, unsubstituted Cp); 5.16, 5.48, 5.91, 5.98, 6.04, 6.30 (each signal: 1H, pseudo s, substituted Cp); 6.86, 7.41 (each signal: 2H, m, phenyl). $^{13}$C NMR ($CD_2Cl_2$): $\delta$ 78.6, 82.1 (unsubstituted Cp); 74.0, 74.2, 75.2, 77.2, 86.3, 86.5, 87.3, 87.7, 87.8, 88.3 (substituted Cp); 123.5, 123.8, 130.2, 131.0, 140.0, 146.6 (phenyl); not observed, carbenium C.

**X-ray Diffraction. X-ray Analysis of (*R*,*S*)-Ferroceno[2,3-*a*]inden-1-one.** A Siemens P4 diffractometer with graphite-monochromatized Mo K$\alpha$ radiation was used for data collection. General procedures used for the structure solution and refinement have recently been published.[5] The relevant crystallographic data for (*R*,*S*)-ferroceno[2,3-*a*]inden-1-one, the synthetic precursor to **10**, are summarized in Table 1 and shown graphically in Figure 1. For complete crystallographic data, see Supporting Information.

**Mössbauer Studies.** The $^{57}$Fe Mössbauer parameters of the subject compounds were determined by standard transmission geometry spectrocopy, using a 50 mCi $^{57}$Co in rhodium source at room temperature. Optically thin ($t < 0.5$) absorbers were prepared by mixing the samples with boron nitride (to effect random sample orientation relative to the optical axis), packing the resulting powders into plastic sample holders, and clamping these, in turn, into a Ricor variable-temperature cryostat. Temperature control in the range $85 < T < 280$ K was effected using a compensated thermocouple-controlled feedback circuit and is stable to ±0.5 °C over the time intervals required to accumulate at least $10^6$ counts/channel in the 256-channel spectrum. Spectrometer calibration was effected using an 18.8 mg cm$^{-2}$ natural iron foil absorber at room temperature, and all isomer shifts are reported with respect to the centroid of this spectrum.

## Results and Discussion

For the sake of clarity and convenience, the structures of compounds **1**−**10** relevant to this study are summarized in Chart 1. The preparation and chemical properties of **1**−**7** have been described elsewhere[5,6,13] or will be published in due course.[14] Compounds **8**−**10** were synthesized as outlined in Scheme 1, essentially in analogy to other metal carbonyl-stabilized carbenium ions.[5,7,8] The chemical stability of the two cations **8** and **9** is far less (slightly air-sensitive, decomposition in solution) in comparison to all-ferrocenyl-substituted systems,[5] indicating the superior donor capability of ferrocene vs metal carbonyl clusters. Compound **10** was prepared from (*R*,*S*)-ferroceno[2,3-*a*]inden-1-one,[18] whose racemic nature was proven by an X-ray single-crystal structure determination (Figure 1 and Table 1, Supplementary Information). Cation **10** is of a stability similar to that of the allylium ion **7**, the [2]cumulenic ion **5**, and the [4]cumulenic ion **6**, which are all air-stable and represent the most stable or only examples of such systems.

**Neutral Compounds 1−4.** The Mössbauer spectra of the neutral tetraferrocenylethane, **1**, as well as the three neutral ferrocenyl-substituted conjugated compounds **2**−**4**, consist of well-resolved doublets having a mean line width of 0.281 ± 0.008 mm s$^{-1}$ at 90 K. A representative spectrum is shown in Figure 2. Not surprisingly, all four ferrocenyl groups are (within the resolution of the Mössbauer technique) identical, and the four metal centers are treated as a single entity in the subsequent discussion, in consonance with the NMR (solution) data for **2**−**4**, which show the 20 protons on the nonbonded Cp groups to be magnetically equivalent in **2**−**4**[6,20] but in contrast to NMR data for **1**,[13] where two signals were observed. We also note that tetraferrocenylethane (**1**)[13,21] and tetraferrocenylethylene (**2**)[6] are both chiral molecules due to severe steric congestion (although only the racemic mixtures are available), whereas the cumulenes (**3**) and (**4**) are achiral,[6] because there is no such steric hindrance. On the other hand, these two cumulenes differ in their molecular shape: the [2]cumulene (**3**) has its two pairs of (syn/anti) ferrocenyl substituents in orthogonal planes to each other, and in the [3]cumulene (**4**), these two pairs of ferrocenyl substituents are in the same plane.

The IS and QS parameters are summarized in Table 2 and are very similar to those reported for the parent ferrocene. It has been noted numerous times in the pertinent literature[9,10] that ring substitution has only a minor effect on the hyperfine interaction parameters of the iron atom in ferrocene-related materials, and this observation is, once again, confirmed by the present results. The QS of the $\sigma$-bonded ferrocenyl substituent is smaller by ∼0.09 mm s$^{-1}$ at 90 K than is observed for the parent ferrocene, but this parameter is only very weakly temperature dependent. The temperature dependence of the IS parameter was extracted from the Mössbauer data, and a typical data set (for **4**) is shown in Figure 3, in which the linear correlation coefficient is 0.997 for the 10 data points. The standard deviation is 0.0019, and is shown by the error bars in

(20) Schütte, D.; Oeser, T.; Irngartinger, H.; Wiesler, M. *Tetrahedron Lett.* **1995**, *36*, 5163.
(21) Denifl, P.; Hradsky, A.; Bildstein, B.; Wurst, K. *J. Organomet. Chem.* **1996**, *523*, 79.

**Chart 1.** Schematic Overview of Structures of the Compounds Investigated[a]

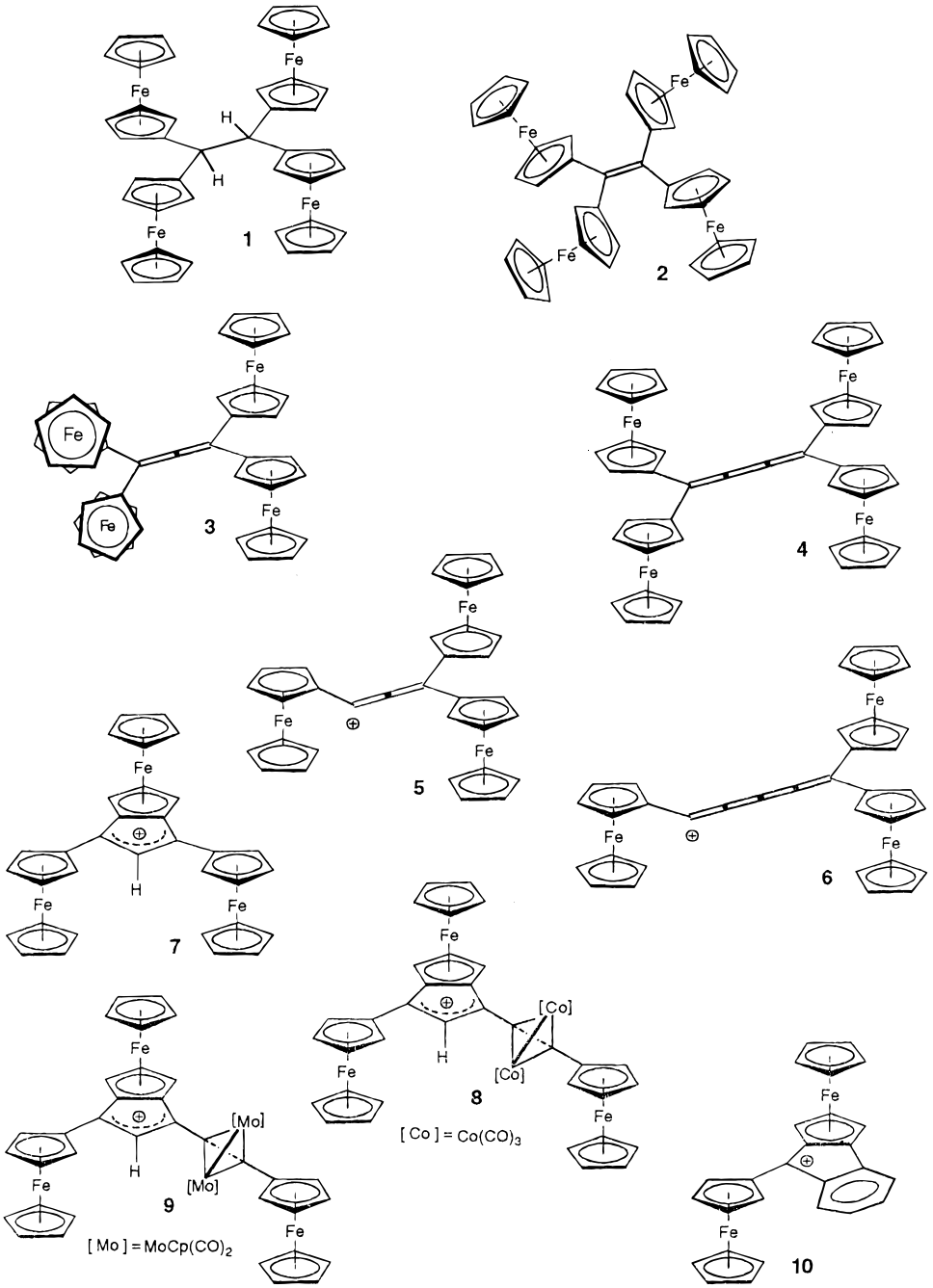


[a] Counterions omitted for clarity.

the figure. The temperature dependence of the isomer shift of the ferrocenyl substituents is very close to that of the parent molecule, leading to an "effective mass"[22] close to that of the parent (105 ± 3 Da). The difference between this parameter and the "bare iron" value of 57 Da is a reflection of the covalent bonding of the metal atom to the $\eta^5$-cyclopentadienyl rings.

In contrast, the QS parameter is only weakly temperature dependent in all of these compounds, since the shape of the electric charge distribution around the metal atom is primarily due to metal−Cp ring interactions, and this is not sensitive to ring substitution effects or to thermal expansion processes.

It is most instructive to compare the lattice dynamical results for **1** and **2** since detailed X-ray diffraction data have been reported for both compounds.[6,13,20,21] The temperature dependence of the recoil-free fraction, which is given by the temperature dependence of the area under the resonance curve for an optically "thin" absorber, is smaller by ∼25% than the value observed for the ferrocene parent and reflects the influence of the $\sigma$ bond to the hydrocarbon fragment on the vibrational modes of the ferrocenyl moiety. A comparison of the temperature dependence of the recoil-free fractions in **1** and **2** is shown in Figure 4. The correlation coefficients are 0.995 and 0.998, and the standard deviations are 0.001 86 and 0.002 13, respectively, as shown by the error bars in the figure. Since the carbon−carbon bond distance is 151.6 pm in **1** (ref 21; see also ref 13) compared to a value of 138.1 in **2**,[6,20] it might have been expected that the temperature dependence would be *smaller* in the ethene than in the ethane complex, arising from a "stiffer" C=C bond. However, just the opposite is observed ($-7.54 \times 10^{-3}$ vs $-6.08 \times 10^{-3}$ K$^{-1}$, respectively). As noted above, both

(22) Herber, R. H. In *Chemical Mossbauer Spectroscopy*; Herber, R. H., Ed.; Plenum Press: New York, 1984; Chapter VII.

**Scheme 1.** Synthesis of Compounds **8**−**10**

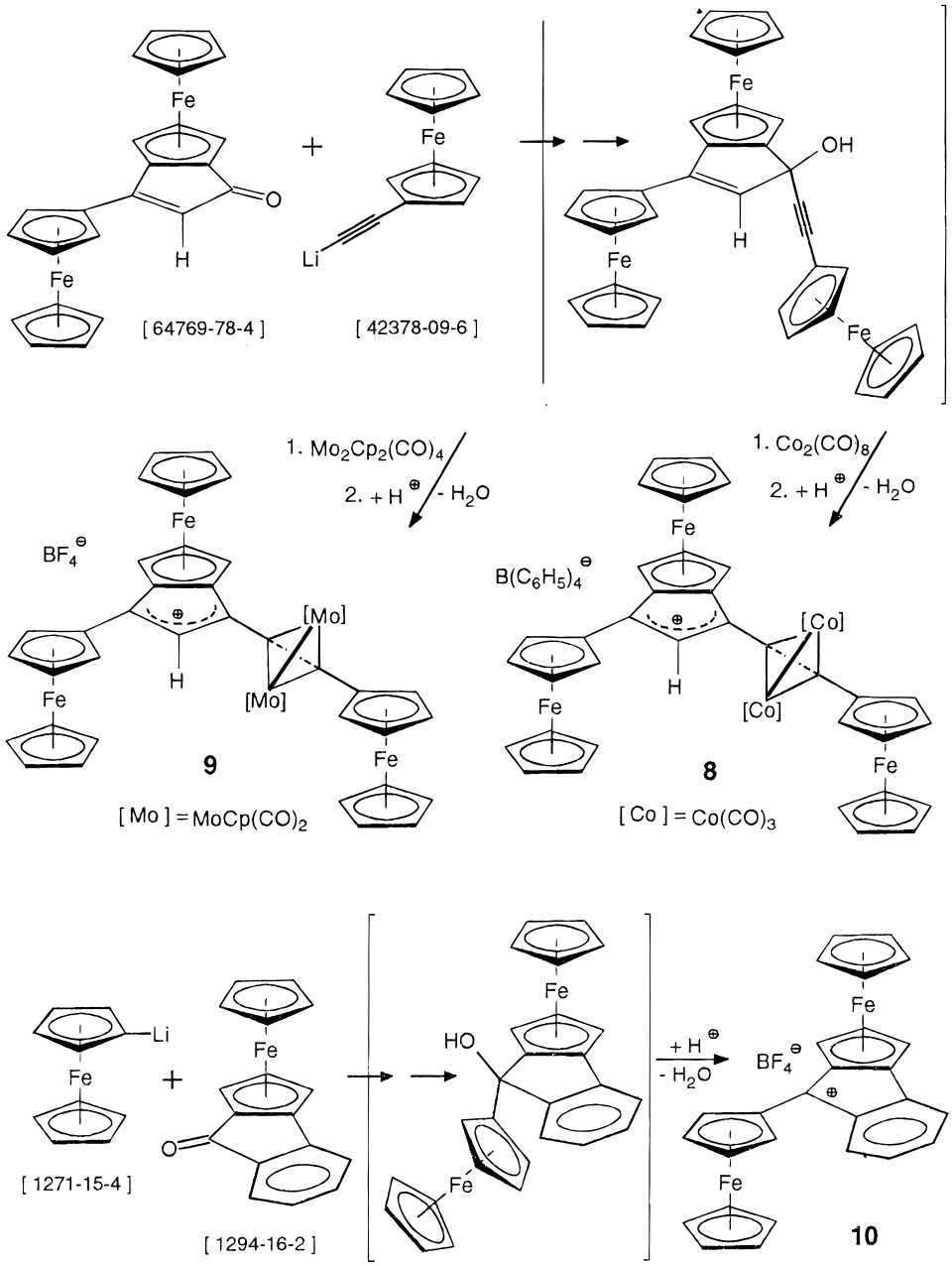


compounds are chiral due to steric crowding of the ferrocenyl substituents and the degree of repulsive interactions seems to be stronger in the $sp^3$-bridged tetraferrocenyl compound **1** in comparison to the $sp^2$-bridged tetraferrocenyl compound **2**, as is evidenced by the observation of two signals for the unsubstituted cyclopentadienyl rings in the $^1H$ NMR spectrum of **1**, whereas for **2** only one resonance can be detected. Notwithstanding these small differences in the d ln $A$/d$T$ parameter between the several neutral compounds, it is clear that this parameter is not sensitive to the number of carbon−carbon double bonds interposed between the two terminal C atoms ligated to the ferrocenyl groups, as is evident from the data for **3** and **4** (Table 2), which differ by one C═C. The clear implication of this observation is that *the motion of the "sandwiched" iron atom is almost completely determined by the metal*−$C_p$ *ring interaction and is not at all sensitive to the vibrational motion of the olefinic framework of the solid.* This generalization turns out to be crucial in achieving an understanding of the behavior of the related cations, *vide infra*.

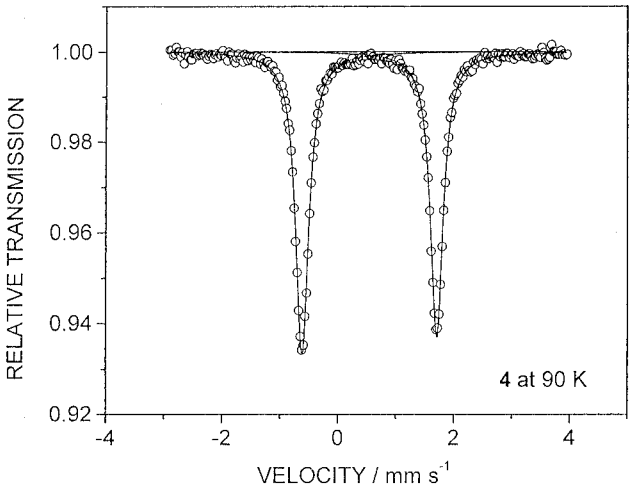


**Figure 2.** $^{57}Fe$ Mössbauer spectrum of **4** at 90 K. The velocity scale is with respect to the centroid of a room temperature spectrum of α-Fe(0).

**Table 2.** $^{57}$Fe Mossbauer Parameters for the Compounds Discussed in the Text[a]

| | | | | | 5 | | 6 | | 7 | | 8 | | 9 | | | | | |
|---|---|---|---|---|---|---|---|---|---|---|---|---|---|---|---|---|---|---|
| | **1** | **2** | **3** | **4** | site 1 | site 2 | site 1 | site 2 | site 3 | site 4 | site 3 | site 4 | site 1 | site 2 | **10** | | $Fe(Cp)_2$ | $Fe(Cp)_2^+BF_4$ |
| IS, mm s$^{-1}$ (90 K) | 0.511 | 0.541 | 0.534 | 0.545 | 0.532 | 0.502 | 0.528 | 0.488 | 0.508 | 0.492 | 0.534 | 0.508 | 0.540 | 0.469 | 0.528 | 0.507 | 0.530 | 0.545 |
| QS, mm s$^{-1}$ (90 K) | 2.341 | 2.328 | 2.355 | 2.322 | 2.156 | 0.527 | 2.202 | 0.687 | 2.089 | 1.453 | 2.264 | 1.425 | 2.190 | 1.389 | 2.039 | 1.583 | 2.428 | |
| d IS/d$T$, mm s$^{-1}$ × 10$^4$ | 3.759 | 4.108 | 3.469 | 3.874 | 3.907 | 5.471 | 3.321 | 3.129 | 2.393 | 2.621 | 3.319 | 3.72 | | | 4.028 | 3.364 | 3.283 | 7.03 |
| d ln [$A(T)$/$A$(90)], mm s$^{-1}$ × 10$^3$ | 6.075 | 7.540 | 5.985 | 6.062 | 9.454 | | 7.680 | | 11.38 | 6.37 | 10.21 | 4.67 | | | 10.35 | 10.56 | 8.66 | |
| $M_{eff}$, Da | 111 | 101 | 120 | 107 | 106 | 76 | 125 | 133 | 174 | 159 | 125 | 130 | | | 103 | 124 | | |
| $\Theta_M$, K | 108 | 102 | 104 | 109 | | | | | | | | | | | 85 | 77 | | |

[a] The uncertainties in the IS and QS parameters are ±0.005 mm s$^{-1}$. The IS($T$) and ln $A(T)$ data were obtained from linear regressions as noted in the text, with correlation coefficients of ~0.989 and 0.997, respectively. Error bars in the figures are indicated where appropriate.

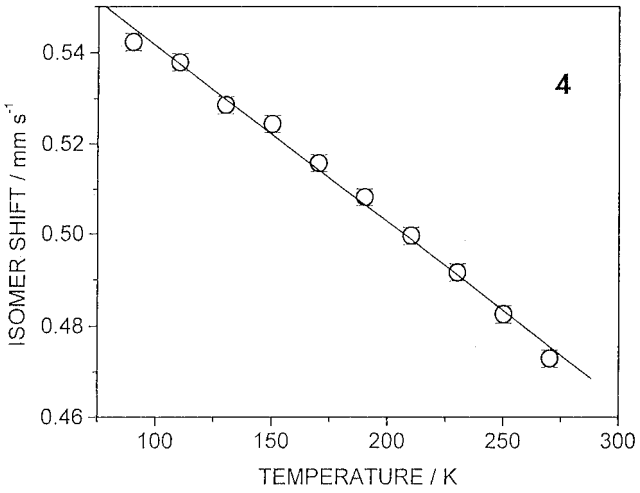


**Figure 3.** Temperature dependence of the IS parameter for **4**. The line is a linear least-squares regression fit to the data. From the slope of this line it is possible to calculate $M_{eff}$ for the iron atom(s) in the sample.

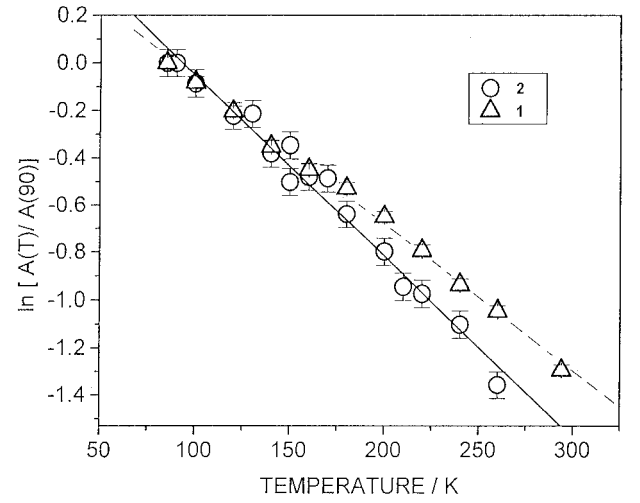


**Figure 4.** Comparison of the temperature dependence of the recoil-free fraction for the iron atoms in **1** and **2**. The lines are linear least-squares fits to the dara. The difference in the two slopes is ~24%.

Finally, it is worth noting that in none of these compounds can a vibrational anisotropy (Gol'danskii−Karyagin effect)[23] be extracted from the temperature-dependent spectroscopic data, even though the ring planes are (nearly) coplanar, and a 5-fold symmetry axis perpendicular to these planes passes through the

(23) Gol'danskii, V. I.; Gorodinskii, G. M.; Karyagin, S. V.; Korytko, C. A.; Krizhanskii, L. M.; Makarov, E. F.; Susdalev, I. P.; Khrapov, V. V. *Proc. Acad. Sci. USSR, Phys. Chem. Sect.* **1963**, *147*, 766. Karyagin, S. V. *Ibid.* **1964**, *148*, 110.

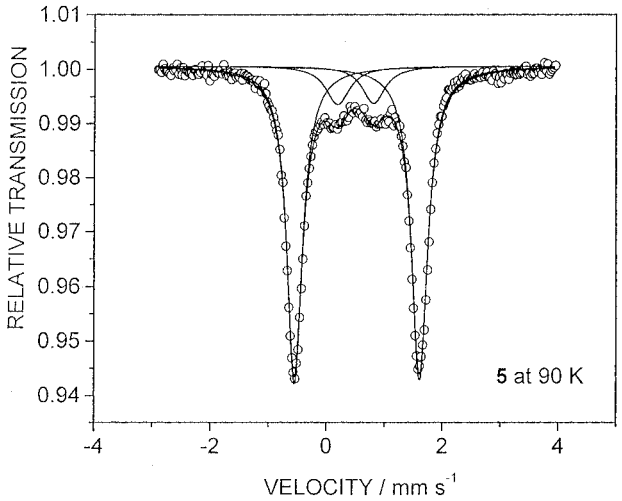


**Figure 5.** $^{57}$Fe Mössbauer spectrum of **5** at 90 K. The spectral data were fit to two quadrupole split resonances (inner and outer), as discussed in the text.

metal centers. As a result of the random orientation of the sample in the spectrometer, no significant temperature-independent intensity asymmetry is observed.

**Cumulenic Carbocations 5 and 6.** The effect of (formally, but not synthetically) removing a ferrocenyl anion from these neutral complexes can be elucidated by a comparison of the Mössbauer results for **5** and **6**, since the latter is the trisferrocenyl carbocation homologue of the former. The Mössbauer spectrum of **5** (Figure 5) at 90 K consists of a more intense doublet (site 1) and a less intense doublet (site 2), having almost the same IS but very different QS parameters (see Table 2). That the site 2 resonance does not arise from a ferricinium-like artifact can be concluded from the fact that the diamagnetic NMR spectra for **5** [5] and **6** [14] show unshifted, sharp lines, indicating that any paramagnetic impurities must be below the 1% level. The temperature dependence of the IS parameter is nearly the same for both sites, leading to similar $M_{eff}$ values. The isomer shift of the site 2 iron atom is ~0.03 mm s$^{-1}$ smaller than that of the site 1 atom, implying a slightly larger s-electron density at the metal center in the former compared to the latter. It is tempting to associate site 2 with the iron atom near the location of the cationic charge, since the QS interaction in these compounds is strongly dependent on the population of the metal orbitals ($d_{x^2-y^2}$ and $d_{z^2}$) directed toward the Cp rings. However, this simple interpretation is clouded by the fact that the area ratio ($R$ = site 2/site 1) under the resonance curve is temperature dependent and is significantly less than the value 0.5 expected at low temperatures if the relative site population is 1:2 as predicted from the structure. The area under the resonance curve is dependent not only on the relative number of metal atoms

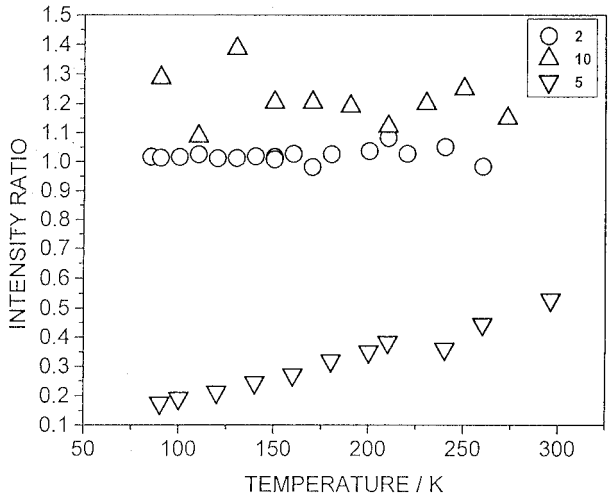


**Figure 6.** Comparison of the temperature dependence of the intensity (area) ratio of the two quadrupole split resonances in **2**, **5**, and **10**. The "anomalous" temperature dependence of this ratio for **5**, as compared to its temperature insensitivity in **2** and **10**, is clearly evident from the data.

**Scheme 2.** Schematic Representation of the two Contributing Structures (Propargylic and Cumulenic Forms of Carbons α, *β*, and *γ*) for **5**

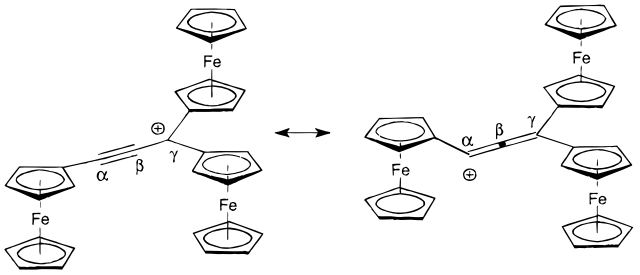


occupying each site but also on the recoil-free fraction parameter, which is, in turn, dependent on the mean square amplitude of vibration of the metal atom. The larger this amplitude (the "softer" the chemical bond) the greater will be the temperature dependence. As noted above, the *a priori* expectation is that d ln *A*/d*T* will be essentially the same for all ferrocenyl groups, regardless of the architecture of the rest of the molecule. Clearly, this is not what is observed in the case of the cationic cumulenes **5** and **6**.

In examining the detailed spectroscopic results for **5** and **6**, the following observed facts need to be accounted for (a) the IS and QS parameters observed and the differences in these parameters for the site 1 Fe atom and the site 2 Fe atom; (b) the observation that the *R* ratio (site 2/site 1) is less than the expected value of 0.5 at low temperatures (see Figure 6); (c) the temperature dependence of the *R* ratio (see Figure 6); (d) the large line width of the site 2 resonance lines; and (e) the differences observed in the apparent d ln *A*/d*T* parameters for the ferrocenyl groups in these complexes and those noted earlier for the neutral species.

A possible rationalization of these observables may be the following: At low temperatures, the ferrocenyl group ligated to $C_\alpha$ (see Scheme 2) causes electron flow into the $p_z$ orbital of $C_\beta$ which then transfers charge, via a $\pi_z$ back-bonding interaction back to $C_\alpha$. This electron flow increases the triple-bond character of the $C_\alpha-C_\beta$ bond, reduces the cationic charge on $C_\alpha$, and makes the ferrocenyl$-C_\alpha$ $\sigma$ bond nearly indistinguishable from a normal ferrocenyl C atom $\sigma$ bond. The IS and QS parameters of this ferrocenyl group are thus indistinguishable from the values associated with the ferrocenyl groups $\sigma$-bonded to the $C_\gamma$ atom of **5**, and its $\gamma$-ray resonance absorption is coincident with the site 1 absorbances in the spectrum. As the temperature increases, motion of the ferrocenyl group relative to the long axis of the molecule interferes with this electron delocalization, and the $C_\alpha$ atom carries an increasing positive charge. The ferrocenyl group ligated to this cationic center (site 2, $C_\alpha$) gives rise to a much smaller QS interaction, and the relative *R* value increases, not only because of the increase in the smaller QS signal but, concommitantly, by the decrease in the larger QS signal. Thus, the apparent d ln *A*/d*T* reflects not only the normal *f*-factor *T* dependence but also the depopulation of the low-temperature conformation of the ferrocenyl group. This interpretation, that the smaller QS signal arises from a ferrocenyl group ligated to a C atom carrying a cationic charge, and hence which will have a distribution of orientations in space relative to the pseudo-$C_{2v}$ axis of the rest of the molecule, also accounts for the large line width of the smaller QS resonance, since this reflects a distribution of QS values around a mean. Thus, the two contributing structures for **5** are those shown in Scheme 2, in which the low temperature form has a major contribution from the ethynyl structure, whereas the cumulenic form contributes increasingly at higher temperatures. This is in agreement with the observation that the room temperature IR spectrum shows only a very strong cumulenic band and no ethynyl vibration. This does not mean that at room temperature only the cumulenic structure obtains, because the ethynyl vibrations (expected in the range 2260−2100 $cm^{-1}$) are known to be very weak and may also be overlapped by the strong cumulenic band. This unfavorable situation also prevented the observation of a relative decrease of the cumulene absorption and increase in the ethyne absorption by variable-temperature (78−293 K) IR spectroscopy. It is interesting to note that analogous effects of temperature and pressure on the dynamics of similar molecular rotors has recently been demonstrated by Silver *et al.*[24]

Finally, it is worth noting that the difference in the temperature dependence of the IS parameter associated with the smaller QS signal is only 25% larger than d IS/d*T* of the larger QS signal, while the apparent (but not real) temperature dependencies of the area under the resonance curve (d ln *A*/d*T*) differ by more than a factor of 2.3 for **5**. The former follows from the fact that $M_{eff}$ is nearly the same for the two ferrocenyl group bonding environments, while the "depopulation" of the larger QS signal resonance (as above) accounts for the anomalously large temperature dependence of the area under the resonance curve, relative to the smaller QS signal doublet.

**Annelated Carbocations 7−10.** The Mössbauer spectrum of **7** provides a key to the understanding of the spectroscopic data for the other annelated, fused ring compounds examined in the present study. It is immediately seen (see Figure 7), that the $^{57}$Fe spectrum of this compound again consists of two distinct doublets, having almost the same IS but distinctly different QS parameters (see Table 2). A detailed single-crystal X-ray structural analysis of this compound has been reported[5] and clearly differentiates the two different kinds of ferrocenyl groups present in this molecule. All of the Cp rings are aligned in the same direction and are parallel to the pentalene ring plane.

Since two of the ferrocenyl ligands are ligated by a single $\sigma$ bond, while the third group is part of the fused ring portion of the molecule, it seems logical to associate the more intense doublet to the former two (site 3) and the latter to the less intense doublet (site 4). In contrast to the results cited above (**5**, **6**) in the case of **7** the area ratio at 90 K is, in fact, very close to that

(24) Silver, J.; Roberts, R. M. G.; Davies, D. A.; McCammon, C. A. *J. Chem. Soc., Chem. Commun.* **1996**, 11.

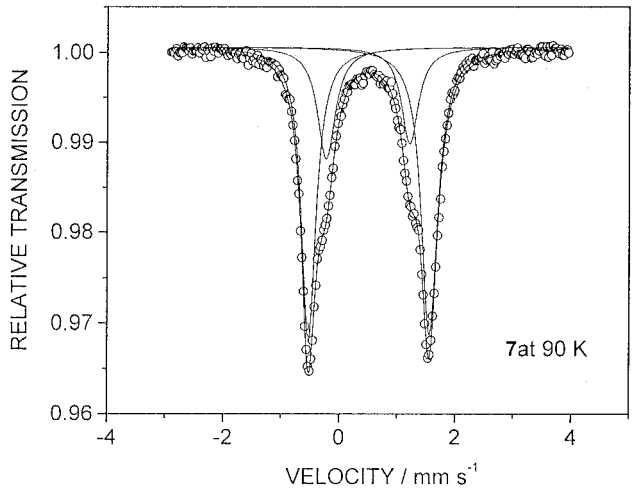


**Figure 7.** $^{57}$Fe Mössbauer spectrum of **7** at 90 K. The data were fit to two quadrupole split resonances. The area ratio is ∼0.51 (site 4/site 3) at 90 K and is temperature independent.

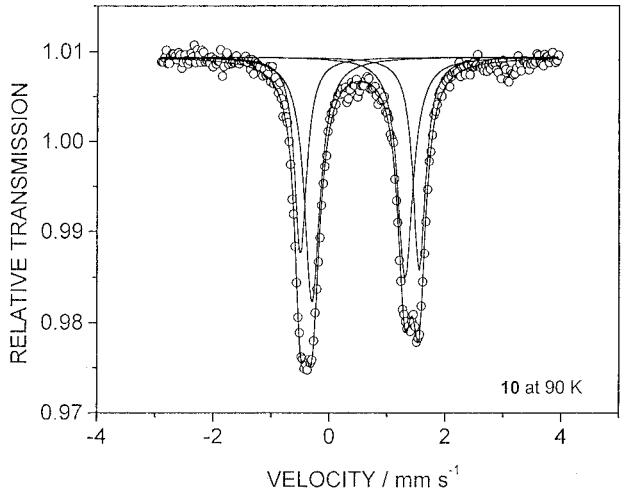


**Figure 8.** $^{57}$Fe Mössbauer spectrum of **10** at 90 K. The data were fit to two quadrupole split resonances. The area ratio is ∼1.2 at 90 K, and is temperature independent in the range $\leq T \leq 273$ K; see also Figure 5.

expected from this assignment (0.51) and is nearly temperature independent to 200 K. Above this temperature, the area ratio increases as noted above, again due to the differences in the *T* dependence of the recoil-free fractions. According to the single-crystal structure analysis[5] the two site 3 groups are, in fact, slightly different, with unequal bending from the pentalene plane, but this difference cannot be resolved from the Mössbauer data. As noted above, the IS of the site 4 iron atom is smaller (at 90 K) by ∼0.016 mm s$^{-1}$ than that assigned to the site 3 metal atom, indicative of a larger electron density at the Fe center in the former than the latter. The QS parameter of the site 3 atom is larger by ∼50% (2.089 vs 1.435 mm s$^{-1}$ at 90 K), and both are nearly temperature independent over the range $90 < T < 280$ K. It is interesting to note that the temperature dependence of the recoil-free fraction of the site 3 metal atom is larger by a factor of ∼2 than that for the site 4 metal atom, again indicative of a "softer" ligation of the ferrocenyl group which is only $\sigma$-bonded to the fused ring portion of the molecule, compared to the site 4 group. Finally, it is worth noting (*vide infra*) that the line width of the inner doublet (site 4) is slightly larger than for the outer doublet (0.32 vs 36 mm s$^{-1}$) despite the prediction that might have been made on the basis of the crystallographic results, but this line width difference is much smaller than in the case of **5** and **6**, as discussed above. In other words, the mechanism of line broadening due to ferrocenyl group rotation around the $C_\alpha$ $\sigma$ bond, which is presumed present in **5** and **6**, appears to be absent in **7**.

Turning next to the spectroscopic results for **8**, it is seen (Table 2) that the Mössbauer parameters are very similar to those for **7**, although there is a significant difference in their temperature dependencies. The former observation implies that the interposition of an ethyne $Co_2(CO)_6$ group between the annulated five-membered ring and the ferrocenyl moiety has little effect on the electron density and the symmetry of the charge distribution around the Fe center and that the two $\sigma$-bonded $FeCp_2$ groups (site 3) are thus spectroscopically identical. The area ratios for the two iron resonances are close to the expected value of 0.5 and are temperature independent in the range $90 \leq T \leq 160$ K. The ratio of the QS parameters for the two sites is ∼1.6. As was true for **7**, the temperature dependence of the recoil-free fraction of the site 3 iron atom is significantly larger (by a factor of ∼2.2) than that of the site 4 Fe atom, again indicating a "looser" bonding of the iron atom in the former than the latter.

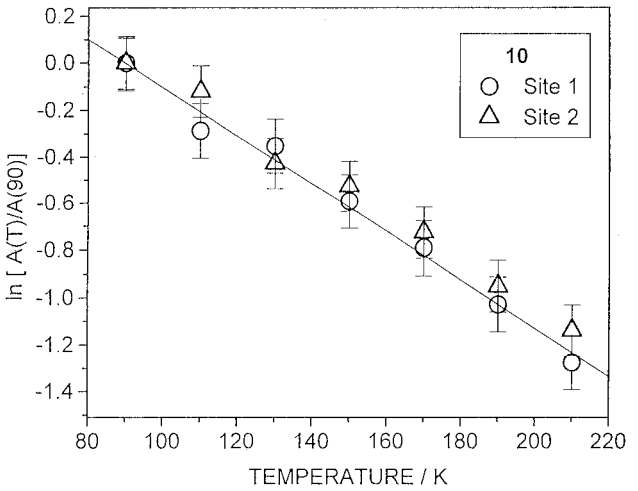


**Figure 9.** Comparison of the temperature dependence of the recoil-free fraction of the two iron sites in **10**. The two slopes are essentially identical (within experimental error), reflecting the insensitivity of the *f* parameter to the difference in ligation mode of the ferrocenyl moiety to the rest of the molecule.

The spectroscopic hyperfine parameters at 90 K for the closely related compound **9**, which differs from **8** by the interposition of a $Mo_2(CO)_4(Cp)_2C_2$ group instead of an ethyne $Co_2(CO)_6$ bridge, are included in Table 2. Again, there is a small (∼0.071 mm s$^{-1}$) difference in the IS parameter and a much larger (∼0.80 mm s$^{-1}$) difference in the QS parameter at 90 K for the two sites. The intensity ratio of the two sites is ∼2.25 at 90 K, close to the value expected from the molecular architecture. However, as indicated by NMR measurements, this sample incorporates one (or more) paramagnetic impurities. In the Mössbauer spectrum at 90 K, one of these broad impurity lines (at ∼0.5 mm s$^{-1}$) overlaps strongly with the "inner" doublet, and hence it was not possible to extract meaningful *T*-dependent data for this sample.

The Mössbauer spectrum of **10** is shown in Figure 8 which again evidences two distinct resonances, having nearly the same IS, but resolvably different QS parameters (see Table 2). The intensity ratio is close to 1:1, as expected, and is not strongly temperature dependent (see Figure 6). Both the presence of only two distinct iron-containing groups, and the values of the hyperfine parameters of **10** permit drawing conclusions related to the mean-square amplitude of vibration (and its temperature

dependence) of the ferrocenyl groups $\sigma$-bonded to the five-membered annelated ring (site 1) and that fused to this ring (site 2). This comparison is summarized in Figure 9, in which the normalized ln [*A*] parameter for the two sites is shown as a function of temperature. The two slopes are $-10.35 \times 10^{-3}$ and $-10.56 \times 10^{-3}$ K $^{-1}$ for sites 1 and 2, respectively. It is thus fair to conclude that the iron atom motion is quite insensitive to the ligation mode of the cyclopentadienyl ring in these complexes over the temperature range of the present data ($90 \leq T \leq 270$ K). Again, this conclusion has direct bearing on the use of ferrocene and ferrocenyl compounds as dynamical probes of complex molecules.[12]

In comparison to **7** and **8**, in which the QS ratio of the two sites is 1.5 and 1.6, respectively, at 90 K, for **10**, this ratio is only 1.3, reflecting the electron demand of the second ferrocenyl-containing moiety ligated to the fused five-membered ring in the former.

## Summary and Conclusions

From $^{57}$Fe Mössbauer studies in the temperature range $90 \leq T \leq 295$ K, the following conclusions can be reached:

(a) For neutral polyferrocenyl ethane, ethylene, and cumulenes, the IS and QS parameters are not sensitive to the details of the carbon framework architecture. The $M_{\text{eff}}$ is $110 \pm 8.0$ Da, and $\theta_{\text{M}}$ is $106 \pm 3.0$ K, similar to its value in ferrocene, and clearly shows that the dynamics of the iron atom are governed by the bonding to the two Cp rings and not by the rest of the molecule.

(b) For polyferrocenyl cumulenic carbocations, two iron sites are distinguishable. The IS of the site closest to the cationic charge ($C_\alpha$) is smaller by $0.035 \pm 0.005$ mm s$^{-1}$, indicative of a slightly larger electron density at the iron atom, and has a QS which is a factor of $\sim$3.7 times smaller than the QS of the iron atoms at the distal sites ($C_\gamma$).

(c) For fused ring (annelated) polyferrocenyl carbocations, two iron sites are distinguishable. The ferrocenyl moieties bonded by a fused ring interaction have an isomer shift (at 90 K) which is 0.016 mm s$^{-1}$ smaller than the iron atom of the $\sigma$-bonded ferrocenyl group(s), and has a QS which is smaller by a factor of $\sim$1.5. The two kinds of iron sites have essentially the same *f* factors, but their Mössbauer signatures permit a ready identification of the differences in the two sites.

**Acknowledgment.** We thank Prof. Karl-Hans Ongania from the Department of Organic Chemistry, University of Innsbruck, for FAB mass spectroscopy. This research was supported in part by the U.S. Israel Bi-National Science Foundation and by the European HCM project "Electron and Energy Transfer in Model Systems and their Implications for Molecular Electronics" (Grant CHRX-CT94-0538).

**Supporting Information Available:** An X-ray crystallographic file in CIF format for the structure of (*R*,*S*)-ferroceno[2,3-*a*]inden-1-one is available on the Internet only. Access information is given on any current masthead page.

IC9614226